COLLISIONAL IONIZATION RATES FOR LITHIUM- AND BERYLLIUM-LIKE IONS*

H.-J. Kunze

Department of Physics and Astronomy
University of Maryland
College Park, Maryland 20742

UNIVERSITY OF MARYLAND
DEPARTMENT OF PHYSICS AND ASTRONOMY
COLLEGE PARK, MARYLAND

COLLISIONAL IONIZATION RATES FOR LITHIUM- AND BERYLLIUM-LIKE IONS*

H.-J. Kunze

Department of Physics and Astronomy
University of Maryland
College Park, Maryland 20742

Collisional ionization rates for C IV, N V and O VI as well as for O V and Ne VII are deduced from the time history of spectral lines emitted by these ions in a hot plasma. The plasma (in the electron temperature range 100 eV to 260 eV) is produced in a 15 kJoule theta pinch device, and it is analyzed using the light scattering technique. The results are consistent with theoretical calculations for O VI , and with a semiempirical formula based on theoretical calculations for hydrogenic ions but smaller by factors 1.5 - 2.

---

*Work supported by the Office of Naval Research.

1. Introduction

Cross sections for ionization by electron impact have been measured now for many neutral and some singly ionized atoms[1]. The technique usually employed is the crossed-beam method. With increasing charge such measurements become very difficult. Not only are then the cross sections decreasing rapidly, but it also is more difficult to obtain suitable high-current ion beams. The cross sections for ionization of some doubly ionized atoms[2,3] appear, at present, to be the only ones measured for higher ionization stages. Multiply ionized atoms, however, are important in many laboratory and astrophysical plasmas. In most of these applications only the corresponding rate coefficients are needed. Such ionization rate coefficients can be deduced from the spectroscopic analysis of a well-diagnosed plasma, as was shown for neon ions in a stellarator discharge[4] and for helium-like CV in a theta pinch plasma[5]. (Excitation coefficients have been obtained by this method as well and will be the subject of another paper.) In the following we present ionization rates for ions of the lithium-like and beryllium-like isoelectronic sequences obtained with a theta pinch device.

2. Theoretical Ionization Rates

Theoretical cross sections for ionization from the ground state specifically of lithium-like and beryllium-like ions have been calculated by Trefftz and Malik for O VI and O V using the Coulomb-Born-Oppenheimer method[6] and the distorted wave approximation[7]. Recently, Schwartz[8] calculated the ionization cross sections for O VI for ionization from the ground state as well as from the 2p excited level in the Coulomb-Born II approximation. The calculations include distortion, which was found to increase the cross section by about 22% at 1.5 times the threshold energy and to a lesser extent at lower and higher impact energies (for example only 13% at 5 times threshold).

The reduced cross section of Schwartz for the ionization from the 2s level of O VI agrees to within 10% with the reduced cross section for ionization from the 1s level of a hydrogenic ion of charge Z = 128 as calculated by Rudge and Schwartz[9] in the Born exchange approximation. The reduced cross section for O VI as given by Trefftz[6] shows essentially the same maximum value, however, the peak is shifted to lower energies and her cross section is smaller at higher energies (e.g. by 30% at four times threshold.) Finally, the reduced cross section for ionization from the 2p level as obtained by Schwartz[8] is somewhat larger than that for ionization from the 2s level (by $\sim$31% at 1.125 times threshold and by $\sim$20% at 5 times threshold).

Using an empirical formula with three free parameters Lotz[10] approximated all experimentally determined cross section curves to within 10% and predicted many unknown cross sections. For ions four and more times ionized his formula reduces to one with a single free parameter, and then essentially agrees with the calculations of Rudge and Schwartz[9] for a hydrogen-like ion with high Z-number. Rate coefficients derived from the predicted cross sections[10] have been computed and are tabulated in Ref. 11.

For many applications a simple expression of general validity for the ionization rates would be more desirable. A good starting point[12] is the well-known effective Gaunt factor excitation rate, where the averaged Gaunt factor must now allow, of course, for all electric multipole transitions. Summing over final states and assuming that the Gaunt factor scales proportional to the principal quantum number in order to obtain the correct scaling law, this procedure suggests a rate coefficient for ionization from a state i of the form

$$I_i = A(T) \cdot \frac{n_i}{E_i} \frac{(kT)^{1/2}}{E_i + 3kT} \exp\left(-\frac{E_i}{kT}\right) \quad . \tag{1}$$

Here n_i is the number of electrons in the i-th shell and E_i the ionization energy. Both kT and E_i are in eV. The factor A(T) consists, besides of a constant, essentially of the effective Gaunt factor. If we compare Eq. (1) with the rate coefficients derived from the Born exchange approximation for hydrogenic ions[9] we can deduce the factor A(T). We choose as a $\sim$ 10% fit in the temperature range $1/10\ E_i \leq kT \leq 10\ E_i$

$$I_i \simeq 7.5 \times 10^{-8} \times \frac{\eta_i}{E_i}\left[\left(\ell n \frac{40kT}{E_i}\right)^3 + 40\right]\frac{(kT)^{1/2}}{E_i + 3kT} \exp\left(-\frac{E_i}{kT}\right) \text{ cm}^3/\text{sec} \qquad (2)$$

In the same temperature range these rate coefficients agree with the predictions given by Lotz[11] to within 15% for all ions of the hydrogen, helium, lithium and beryllium isoelectronic sequences of charge greater than three. The above formula approximates the rates for O VI derived from Schwartz's calculations[8] also to within $\sim$ 10%, and agrees with the experimental rate coefficient obtained for helium-like C V[5]. We finally can make a comparision with specific calculations for C V and C VI in the Coulomb-Born approximation[13]. The agreement for C V is very good (to better than 15%), whereas the rates for ionization from the ground state of C VI are larger by about a factor of $\sim$ 1.4 in Ref. 13.

Equation (2) may also yield ionization rates from excited levels. Beigman and Vainshtein[13] calculated the ionization rates from the 2s and 2p level of C VI. Over the whole temperature range $1/10\ E_i \leq kT \leq 10\ E_i$ the rates averaged over s and p levels agree to within 25% with Eq. (2). A similar agreement is obtained for the ionization from the 2s level of hydrogenic ions as calculated in Ref. 9. Equation (2), of course, approximates the 2p-ionization for O VI as calculated by Schwartz to within $\sim$ 20%.

When considering the ground state ionization of lithium-like and beryllium-like ions one might have to account for contributions from the filled 1s shell (see Ref. 11). For large Z these contributions are reasonably well approximated by the rate coefficient for ionization of the corresponding helium-like ion; this can be shown by comparing Eq. (2) for a helium-like ion with the rates for K-shell ionization of

the neutral atom as deduced from measured cross sections[14]. One obtains thus contributions from inner shells smaller than 20%. They can therefore be neglected, at least for most applications where $kT \leq 10\ E_i$.

3. Principle of the Measurements

The principle of the measurements is identical to that used by Hinnov[4]. The atoms of interest are introduced into a plasma which is heated and compressed to desired temperatures and densities. The ions go then successively through the various ionization stages, the degree of ionization lagging behind the corresponding quasi-stationary corona equilibrium. During that time they emit line radiation, the time history of which can be interpreted in terms of desired ionization rate coefficients.

The concentration N_j of the j-th ionization stage is determined by the following rate equation

$$\frac{dN_j}{dt} = NN_{j-1}I_{j-1} - NN_jI_j + NN_{j+1}\alpha_{j+1} - NN_j\alpha_j + \frac{1}{N}\frac{dN}{dt}N_j, \qquad (3)$$

where N is the electron density and α_j the recombination rate coefficient. The last term in Eq. (3) is a source term keeping the total concentration of the ions constant during compression or expansion phases of the discharge. For the plasma conditions used in the present experiment the recombination rates usually are so small that they can be neglected. This simplifies Eq. (3) considerably: the concentrations of the ions are then solely governed by the ionization rates. In Eq. (3) the products N_jI_j represent the sum of the ionization rates from the ground state and all excited levels, among which contributions from metastable levels can be considerable. As was shown for helium-like CV[5], these contributions from

excited metastable levels could be made small by going to low electron densities, so that the ionization occured solely from the ground state. In this limit it is also justified to assume nearly all ions to be in their respective ground states.

For an optically thin allowed line, whose upper level is essentially populated by electron collisions from the ground state, the emission coefficient is given by

$$\varepsilon = \frac{h\upsilon}{4\pi} N \; X \; N_j \; , \qquad (4)$$

N_j now representing the ground state population and X the rate coefficient for excitation from the ground state. If N and X were constant, the time history of the line would reflect exactly the time history of the respective ion. Otherwise, the time variation of N and X can readily be corrected for even if the absolute value of X is not known too accurately. Its time dependence should be presented sufficiently well by the effective Gaunt factor approximation (see for example Ref. 15), at least for the usually small temperature variations occuring during the emission of many of the lines investigated in our plasma. For the solution of Eq. (3) and Eq. (4) one mostly has to know the electron density and temperature. Both were determined using the light scattering technique[16].

With the measured electron density and temperature as input the coupled rate equations (3) were solved using a computer program[17,18]. The ionization rates used were essentially those given by Eq. (2). However, a variable factor R was introduced by

$$I_{ex} = R \; I_i \; , \qquad (5)$$

which was varied until the calculated time histories obtained with Eq. (4) agreed with those of the observed lines.

Especially for higher ionization stages, one has to check whether the neglect of recombination is still justified. Using recombination rates as given by Düchs and Griem,[18] this was found to be the case for our conditions.

We finally have to consider the particular ions being investigated here. Ions of the lithium isoelectronic sequence are characterized by a low-lying $2p\,^2P$ level. With increasing electron density its population will approach the Boltzmann value, and ionization from it would be stronger than from the ground state. At lower densities the population can be obtained by equating collisional rates into that state with radiative and collisional rates out of it. Using excitation rates as given by Bely[19] and by Burke et al.[20], and transition probabilities as given by Wiese et al.[21] one finds, e.g., for extreme conditions in our experiment ($N \sim 7.10^{15}$ cm^{-3}, $T_e \sim 100$ eV) that in this case only ~60% of all NV ions are in the ground state and almost 40% in the excited $2p\,^2P$ level. For higher ions in the isoelectronic sequence the population of this level will be, of course, much smaller.

In general, one will obtain an average ionization rate coefficient (contributions from higher levels being small due to low population densities) given by

$$I_j \approx \frac{N(2s)}{N_j} I(2s) + \frac{N(2p)}{N_j} I(2p) \quad . \tag{5}$$

The ionization from the 2p level can be estimated from Eq. (2). In our experiment the electron temperatures are of the order of the ionization energies of the ions investigated, and the ionization energies for the 2s and 2p levels are also of the same magnitude [$E(2p) \gtrsim 0.8E(2s)$ for CIV and $E(2p) \geq 0.9E(2s)$ for higher ions in the isoelectronic sequence]:

ionization rates from the 2s and 2p level should agree, therefore, for our conditions to within ∿20%. This is suggested both by the theoretical calculations of Schwartz[8] for the ionization of OVI and those of Beigman and Vainshtein[13] for the ionization from the 2s and 2p levels of hydrogenic CVI. The error introduced when interpreting the observed ionization rates as solely due to ionization from the ground state should be negligible, therefore, for our conditions.

We further have to select appropriate spectral lines to observe. As long as the 2p level population is sufficiently small, most upper levels will be populated directly by collisions from the ground state, and lines will reflect the ground state density according to Eq. (4). This does not hold any more, however, for our specific NV example. Here, the strongest channel for populating the 3p and 3d levels is via the 2p level[20]. It is best, therefore, to observe the 3s → 2p transition, the excitation rate 2p → 3s being sufficiently b e l o w the 2s → 3s rate.

More complicated is the situation for beryllium-like ions, which have five low-lying n=2 excited levels, the lowest one being even metastable ($2p\ ^3P$). Due to the large statistical weight (9 compared to 1 of the ground state), its population will usually be much larger than that of the ground state, although it is not established that the Boltzmann value is achieved. For all our experimental conditions the ionization thus occurs mainly from the $2s2p\ ^3P$ metastable level, the average ionization rate being given again by a relation similar to Eq. (6). All further considerations are analogous to those for lithium-like ions;

the ionization rates from the ground state and the $2s2p\,^3P$ level should again be practically the same for our cases. The population of the other low-lying excited levels may be estimated using semiempirical excitation rates (see e.g. Ref. 15). However, they can also be determined experimentally by measuring the absolute intensities of the corresponding lines[22]. One can observe the $2p\,^2\,^3P$-$2s2p\,^3P$ transition, since it is populated primarily from the $2s2p\,^3P$ level and should thus reflect the change in its population. If lines appear to become optically thick, transitions from n=3 levels are also suited; they will be populated from both the ground state and the metastable triplet level.

Finally, the time history of each ionization stage is strongly influenced by the history of the previous ionization stages. For this reason lines from ions of the boron- and carbon-isoelectronic sequences were also observed and their time-dependent intensities matched with computed values.

4. Experiment

The plasma used for our measurements was produced in a theta pinch device, which is described in Ref. 23. For the present experiments it was operated with a stored energy of 15kJ in the main bank. Compared to the description in Ref. 23 the capacitance of the preheater was increased slightly from 0.5μF to 0.7μF; we also increased the damping of the preheater discharge by introducing a damping resistor into the discharge circuit and thus were able to fire the main discharge somewhat earlier.

Three different discharge conditions were investigated; they were obtained by varying the filling pressure, the bias magnetic field and the time Δt between the beginning of the preheater discharge and the ignition of the main bank. The discharge parameters are given in Table I.

Electron densities and temperatures were obtained as a function of radius and time in the midplane of the coil using the light scattering technique. The setup is the same as used in Ref. 5. The absolute sensitivity calibration was done again using the Rayleigh scattering in N_2. (The cross section used was $\sigma_R = 1.73 \cdot 10^{-27} cm^2$). As an example, Fig. 1 gives the electron density and temperature as a function of time on the axis of the discharge tube (r=0) for case (A) as well as the radial profiles at four different time points. Figure 1 also shows the time history of the temperature of CV ions as deduced from Doppler profiles observed side-on in the midplane of the coil. Case (A) is somewhat unfavorable for our measurements, since part of the trapped negative magnetic field exists during the whole first half-cycle of the discharge, resulting in a very stable hole in the plasma. The other cases investigated do not show such holes, the trapped negative magnetic field disappearing quite early in the discharge cycle. At early times of the discharge the plasma column experiences also a strong axial compression, and the length of the plasma column was measured by observing lines of various ionization stages of carbon through equidistant holes in the theta pinch coil.

Spectroscopic observations were made end-on as well as side-on in the mid-plane of the coil. End-on, a vacuum-UV-monochromator of the Seya-mount type and a 2-meter grazing incidence instrument were used. Stops assured that only the center of the plasma column (1.25 cm in diameter) was observed. Side-on observations were made in the visible using a 1/2-meter monochromator. It was quite important to compare end-on and side-on observations. In general, it turned out that the time histories did not agree for the lower ionization stages, the lines observed end-on usually displaying much slower decay rates than the ones obtained side-on. However, with increasing ionization stage the time histories became more and more alike until they agreed for the higher ones, indicating the plasma was then essentially homogeneous as assumed in our analysis.

This situation is readily explicable. The higher ionization stages will exist only in the hot plasma core whereas the lower stages will prevail for some time in cooler or low-density zones at the ends of the plasma column. Here not only plasma is lost, but the axial compression is also not complete and will leave some low-density plasma behind. For this reason, side-on observations were preferred, when suitable visible lines could be found.. Carbon, nitrogen, oxygen and neon ions were investigated. Carbon and oxygen are natural impurities in our plasma, whereas nitrogen and neon were added in small amounts (<1%) to the initial filling gas.

5. Results and Discussion

Table II gives the factor R, which is the ratio of experimental rate coefficient to the theoretical one as given by Eq. (2). Column 2 shows the temperature range over which the ions could be observed in the three cases (A), (B), and (C). Several more cases were investigated, but gave less reliable values.

As mentioned in Section 3, although a constant electron density and temperature would be desirable, some variations of N and T can be accounted for. This, however, is possible only as long as the variations are not too strong. The time history of a line is characterized by the derivative of the intensity $P_j = \varepsilon \cdot \ell$ (ℓ = depth of the plasma along the line of sight),and from Eq. (2) and Eq. (3) one obtains

$$\frac{1}{P_j}\frac{dP_j}{dt} = \frac{2}{N}\frac{dN}{dt} + \frac{1}{X}\frac{dX}{dT}\frac{dT}{dt} + \frac{1}{\ell}\frac{d\ell}{dt} + \frac{N_{j-1}}{N_j} NI_{j-1} - NI_j. \qquad (7)$$

For a good determination of the ionization rates the first three terms should not dominate the time history. Unfortunately, however, they tend to do so for the lower ionization stages, which occur early during the discharge, because then compression and heating of the plasma are very rapid.

For this reason, the values for C IV in Table II are not too reliable and are quoted therefore only in brackets. (For this case it was also not possible to match computed and observed time histories very well.) For similar reasons, no ionization rates for higher stages like Ne VIII were obtained. These ions occur so late during the

discharge cycle that plasma losses become considerable, and it was found that the time history of Ne VIII, for example, was essentially determined by the first term of Eq. (7). In some cases the values of R in Table II could not be varied by more than 20% before deviations of computed and observed time histories of lines became obvious, in other cases this limit was about 50%. The absolute values of the electron density and temperature should be accurate to ∿15%. It is difficult to determine systematic errors introduced, for example, by ions in the low-density plasma outside the hot core. Possible errors due to the fact that during the early compression phases of the discharge ionization of ions occurs already in the high density shock region, while the low ionization stages at the center are still unaffected, have been reduced by using lower "effective" ionization rates for the lower stages. It was estimated that the over-all accuracy of our experimental rates is a factor of 2 or better.

The experimental rate coefficients obtained are only about 60% the theoretical rates given by Eq. (2). However, this is within the experimental accuracy, and these measurements thus not only are in agreement with Eq. (2) but also with the predicted rate coefficients of Lotz[11] and the theoretical calculations of Schwartz[8] for O VI. In addition, possible systematic errors in our measurements as mentioned above would tend to yield too low values.

Acknowledgments

The author would like to express his appreciation to H.R. Griem and O. Bely for valuable discussions, to D. Düchs for one of the two computer programs used, to W.D. Johnston for assistance in the measurements and to S.W. Schwartz for making his calculations available prior to publication. The computer time for this project was supported by the National Aeronautics and Space Administration Grant NsG-398 to the Computer Science Center of the University of Maryland.

REFERENCES

1. L.J. Kieffer and G.H. Dunn, Rev. Mod. Phys. 38, 1 (1966).
2. B. Peart, S.O. Martin and K.T. Dolder, J. Phys. B. (Atom.Molec. Phys.) Ser. 2, 2 , 1176 (1969).
3. Z. Z. Latypov, S.E. Kupriyanov and N.N. Tunitskii, Sov. Phys. JETP 19, 570 (1964).
4. E. Hinnov, J. Opt. Soc. Am. 56, 1179 (1966) and 57, 1392 (1967).
5. H.-J. Kunze, A.H. Gabriel and H.R. Griem, Phys. Rev. 165, 267 (1968).
6. E. Trefftz, Proc. Roy. Soc. A271 379 (1963).
7. F.B. Malik and E. Trefftz, Z. Naturf. 16a, 583 (1961).
8. S.W. Schwartz, to be published.
9. M.R. H. Rudge and S.B. Schwartz, Proc. Phys. Soc. 88, 563 (1966).
10. W. Lotz, Z. Phys. 206, 205 (1967), Z. Phys. 216, 241 (1968).
11. W. Lotz, Astrophys. J., Suppl. 14, 207 (1967) and Report IPP 1/62, Institut für Plasmaphysik, Garching bei München, 1967.
12. H. R. Griem, private communication.
13. I.L. Beigman and L.A. Vainshtein, Sov. Astron. 11, 712 (1968).
14. G. Glupe and W. Mehlhorn, Phys. Letters 25A, 274 (1967).
15. R.C. Elton in Methods of Experimental Physics - Plasma Physics, edited by H.R. Griem and R.H. Lovberg, (Academic Press, New York, to be published 1970).
16. H.-J. Kunze, in Plasma Diagnostics, edited by Lochte-Holtgreven (North Holland Publishing Company, Amsterdam, 1968).

17. G. D. Hobbs and M. A. Rose, Culham Laboratory, Report CLM-R3 (1963).

18. D. Düchs and H.R. Griem, Phys. Fluids 9, 1099 (1966).

19. O. Bely, Proc. Phys. Soc. 88, 587 (1966).

20. P.G. Burke, J.H. Tait and B.A. Lewis, Proc. Phys. Soc. 87, 209 (1966).

21. W.L. Wiese, M.W. Smith and B.M. Glennon, National Bureau of Standards Report No. NSRDS-NBS-4, Vol. 1, 1966.

22. W.D. Johnston III and H.-J. Kunze, to be published.

23. A.W. DeSilva and H.-J. Kunze, J. Appl. Phys. 39, 2458 (1968).

CAPTIONS

Fig. 1. Values obtained as a function of time t, and radius r, from the Thomson-scattering measurements for case (A); (a) for electron temperature T, and (b) for electron density N.

Table I: Discharge Conditions

	filling pressure	bias magnetic field	Δt
A)	11 mTorr H_2	-600 Gauss	15.5 μsec
B)	11 mTorr H_2	-200 Gauss	22.5 μsec
C)	23 mTorr H_2	-600 Gauss	15.5 μsec

TABLE II: Ratio R of experimental to theoretical rate coefficients.

Ion	T_e[eV]	Case (A)	Case (B)	Case (C)	Average
O VI	140 - 260	0.7	0.6	0.6	0.6
N V	120 - 250	0.3	0.6	0.6	0.5
C IV	100 - 150	(0.6)	(0.5)	(0.6)	0.6
				Average	0.6
Ne VII	130 - 260	0.5	0.9	-	0.7
O V	130 - 210	0.4	0.5	0.6	0.5
				Average	0.6

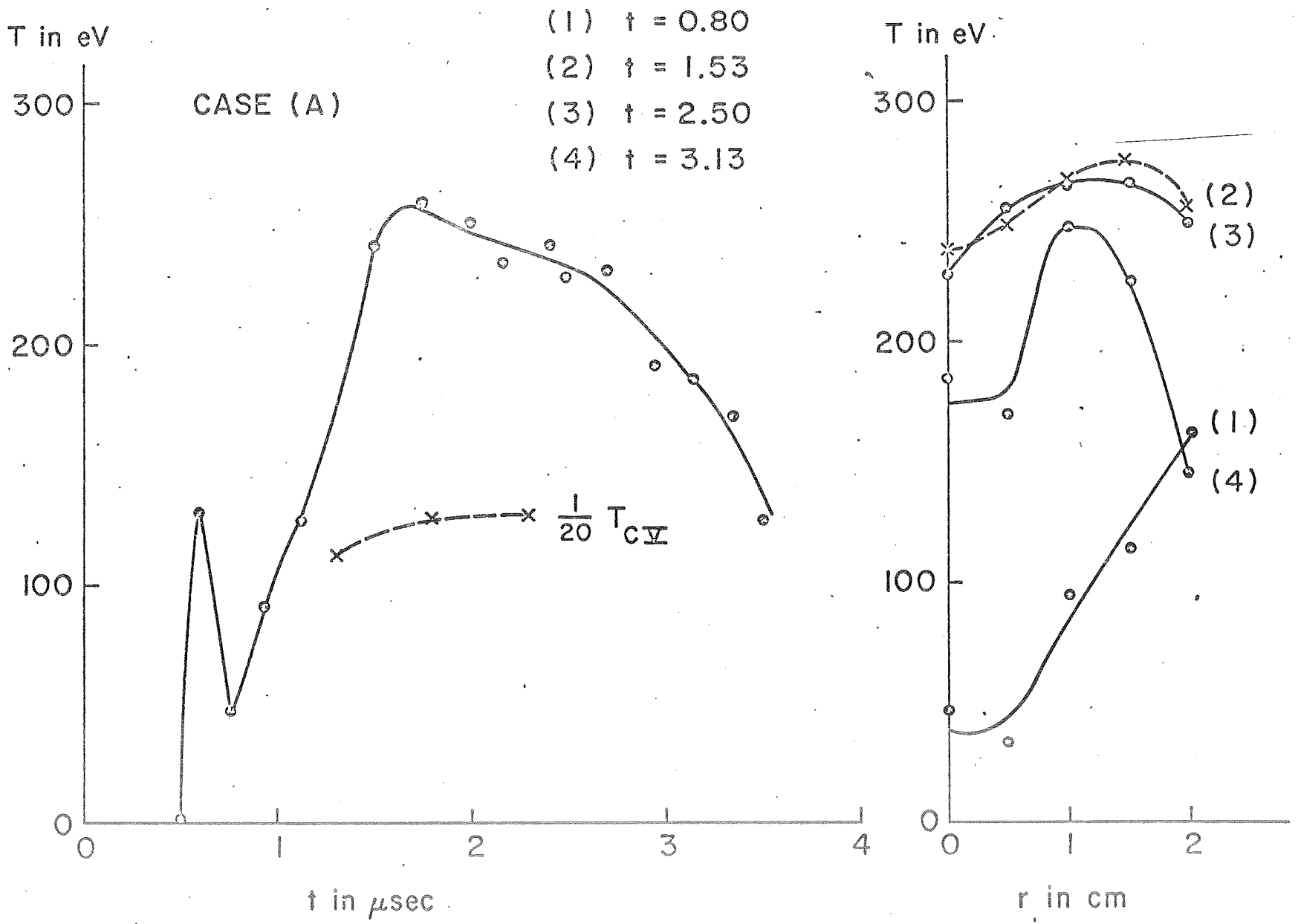
T in eV
CASE (A)
(1) t = 0.80
(2) t = 1.53
(3) t = 2.50
(4) t = 3.13
300
200
100
0
0
1
2
3
4
t in μsec
1/20 T_CV
T in eV
300
200
100
0
0
1
2
r in cm
(2)
(3)
(1)
(4)

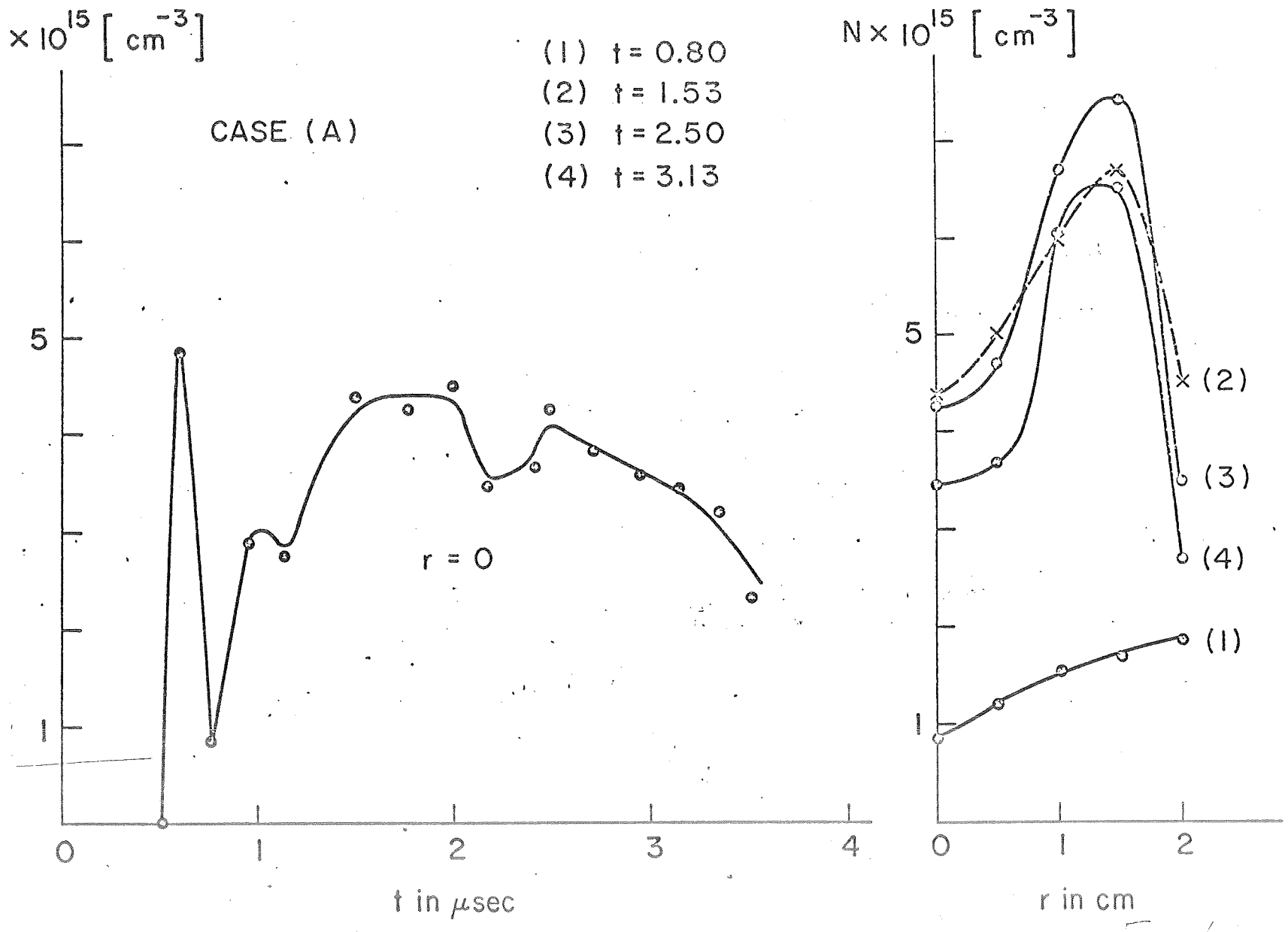
× 10^15 [cm^-3]
CASE (A)
(1) t = 0.80
(2) t = 1.53
(3) t = 2.50
(4) t = 3.13
r = 0
5
1
0
1
2
3
4
t in μsec
N × 10^15 [cm^-3]
5
1
(2)
(3)
(4)
(1)
0
1
2
r in cm